

Depletion of ARGs in antibiotic-resistance *Klebsiella*, *Pseudomonas* and *Staphylococcus* in hospital urines by electro and photo-electro disinfection

Miguel Herraiz-Carboné^a, Salvador Cotillas^{b,*}, Engracia Lacasa^{a,*}, Pablo Cañizares^c,
Manuel A. Rodrigo^c, Cristina Sáez^c

^a Department of Chemical Engineering, Higher Technical School of Industrial Engineering, University of Castilla-La Mancha, Edificio Infante Don Juan Manuel, Campus Universitario s/n, 02071 Albacete, Spain

^b Department of Chemical Engineering and Materials, Faculty of Chemical Sciences, Complutense University of Madrid, Avenida Complutense s/n, 28040 Madrid, Spain

^c Department of Chemical Engineering, Faculty of Chemical Sciences and Technologies, University of Castilla-La Mancha, Edificio Enrique Costa Novella, Campus Universitario s/n, 13005 Ciudad Real, Spain

ARTICLE INFO

Keywords:

Antibiotic-resistant bacteria
Antibiotic resistance genes
Urine
Electrodisinfection
Photo-electrodisinfection

ABSTRACT

The depletion of *bla*_{KPC} (*K. pneumoniae*), *bla*_{OXA-50} (*P. aeruginosa*) and *mecA* (*S. aureus*) genes from hospital urines is evaluated to contribute to solve the silent pandemic of antibiotic-resistance bacteria. A microfluidic flow-through reactor with MMO anode and CB/PTFE cathode working at 50 A m⁻² is employed during electro-disinfection and photo-electrodisinfection processes. The electrodisinfection process only achieves an almost negligible removal of DNA and slightly log ARG increments of 0.18, 0.19 and 0.71 for *bla*_{OXA-50}, *mecA* and *bla*_{KPC} genes, respectively. Conversely, the photo-electrodisinfection process attains the complete disinfection for all ARB tested and logarithmic removals of 3.70, 2.25 and 0.82 for *bla*_{OXA-50}, *mecA* and *bla*_{KPC} genes, respectively. These outcomes emphasize the potential of the UV light coupled to the electrodisinfection process to promote the formation of not only hypochlorite but also chlorine and even nitrogen radicals, which contribute to enhance the disinfection efficiency of the target ARB and their ARGs.

1. Introduction

The alarming spread of antibiotic-resistant bacteria (ARB) has become a global concern due to the significant number of deaths occurring worldwide. The European Centre for Disease Prevention and Control has pointed out the great threat posed by ARB due to 671,689 ARB infections and 33,110 deaths during 2015 [1]. More recently, 2,868,700 ARB infections per year with 24,900 deaths have been estimated in the United States by the U.S. Department of Health and Human Services [2]. Furthermore, the spread of antibiotic resistance genes (ARGs) may also be developed due to vertical transfer (i.e., cell division) and/or horizontal gene transfer processes (conjugation, transduction and natural transformation) [3]. The acquisition of antimicrobial resistance genes (ARGs) by *Staphylococcus aureus* (*S. aureus*), *Klebsiella pneumoniae* (*K. pneumoniae*) or *Pseudomonas aeruginosa* (*P. aeruginosa*) have been reported to reduce the treatment options of severe infections such as pneumonias, sepsis, endocarditis, skin infections, etc. [4–6].

Hospital urines can be considered as one of the main hotspots of ARB and ARGs since microorganisms are excreted from infected patients

mainly by urine [7]. Some studies have recently reported on the pre-treatment of hospital urines to prevent the appearance and spread of ARB, ARGs and mobile genetic elements [8–12]. Conventional technologies based on the addition of chlorine disinfectant species are widely applied in disinfection processes. However, several studies have reported on the increment of ARGs during chlorine disinfection. Wu et al. have recently found that the relative abundance of 14 ARGs (*tolC*, *acrA*, *acrB*, etc.) increased by 49.6 % after the disinfection process with 5 mg dm⁻³ of chlorine [13]. Likewise, Jin et al. reported on the increment of ARGs exchange across bacterial and the emergence of new ARB after the disinfection process with hypochlorite (NaClO in the range 4–6 mg dm⁻³). These results were attributed to the enhancement of horizontal transfer processes by the increment of the cell membrane permeabilisation and a stronger stress-response of the survival ARB [14]. Kampf has also recently reported on the lack of data available in the literature on a possible induction/reduction of antibiotic resistance genes and horizontal gene transfer processes using hydrogen peroxide as a disinfectant [15]. On the other hand, UV disinfection is known to promote bacterial inactivation by damages caused on deoxyribonucleic

* Corresponding authors.

E-mail addresses: salvacot@uclm.es (S. Cotillas), engracia.lacasa@uclm.es (E. Lacasa).

<https://doi.org/10.1016/j.jwpe.2022.103035>

Received 5 June 2022; Received in revised form 8 July 2022; Accepted 28 July 2022

Available online 5 August 2022

2214-7144/© 2022 The Author(s). Published by Elsevier Ltd. This is an open access article under the CC BY license (<http://creativecommons.org/licenses/by/4.0/>).

acid (DNA) and antibiotic resistance genes (ARGs) [16]. However, damages caused by UV disinfection can be repaired after relatively small times, promoting bacterial regrowth [17]. UV irradiation may be coupled to catalysis processes (photocatalysis) to improve the removal of microorganisms from water environment [18]. Venieri et al. reported a 6 log reduction of *Klebsiella pneumoniae* in real wastewater with a binary Co/Mn-TiO₂ catalyst under simulated solar irradiation [19]. *S. aureus* was inactivated during the photocatalysis process using α -NiMoO₄ as catalyst due to the generation of intracellular reactive oxygen species [20].

The electrochemical advanced oxidation processes (EAOPs) provide several advantages for the disinfection treatment, e.g., they are considered as environmental-friendly technologies because the electron is a clean reagent [21,22]. Tu et al. reported a 99.99 % of inactivation SARS-CoV-2 using in-situ formed nickel oxide hydroxide as anode catalyst in the electrochemical oxidation process at 5 V [23]. Simultaneous removal of ARB and ARGs by the electrochemical disinfection have also been carried out in recent literature. Fang et al. achieved 5-log *Escherichia coli* K-12 LE392 removal and, simultaneously, they attained the degradation of *tetA* and *bla*TEM genes by molybdenum carbide assisted electrochemical disinfection under 2 V [24]. Zhang et al. achieved 83.46 % (*Escherichia coli* 10,667 (*su*)) ARGs degradation compared to 10.23 % during chlorination or 27.07 % under UV light irradiation [25]. Additionally, the coupling of UV light with the electrochemical disinfection process may enhance the generation of powerful chlorine and/or nitrogen radicals by the photoactivation of the electrogenerated disinfectants as hydrogen peroxide, hypochlorite or chloramines. Many works have published on the efficiency of different radicals to degrade DNA and ARGs [26–28]. Ahmed et al. evaluated a modified photo-Fenton process at neutral pH and using ethylenediamine-N,N'-disuccinic acid (EDDS) to chelate iron(III) for the removal of ARB and ARGs [26]. They found that 0.1 mM Fe(III), 0.2 mM EDDS and 0.3 mM hydrogen peroxide (H₂O₂) allowed to decrease the concentration of e-ARGs by 6-log within 10 min. Additionally, Zhang et al. studied the oxidative damage induced on ARGs in a novel sulfidated micron zero-valent activated persulfate system. They attributed removals of 2.9 (*TetB*) and 2.2 (16S rRNA) logs to the promotion of reactive oxygen species in the solution, mainly sulfate and hydroxyl radicals [28].

With this background, the main goal is to study the performance of the electrodisinfection and photo-electrodisinfection process for the removal of ARB and ARGs in hospital urines. To do this, the target bacteria were selected based on their potential to cause urinary tract infections (UTIs) in patients from the University Hospital Complex of Albacete (Spain) and, on the sanitary and environmental risk that they posed. A microfluidic flow-through reactor (MMO anode, CB/PTFE cathode) was used during the disinfection tests of hospital urines. A current density of 50 A m⁻² was employed to maximize the efficiency of the electrogeneration of chlorine derived species.

2. Material and methods

2.1. Chemicals and bacterial strains

Compounds employed to prepare the synthetic urine matrix were used as received from Sigma Aldrich, Spain. Arsenic trioxide (Sigma Aldrich, Spain) and sodium hydroxide (Panreac, Spain) were employed for the determination of hypochlorite ion. Potassium phosphate monobasic, sodium phosphate dibasic, ethylenediaminetetraacetic acid (EDTA), N,N-Diethyl-*p*-phenylenediamine sulfate from Sigma Aldrich (Spain), and sulfuric acid from VWR were required for the determination of chloramines. Titanium (IV) oxysulfate solution (Sigma Aldrich, Spain) was employed for the determination of hydrogen peroxide. All chemicals were analytical grade and used as received. Double deionized water (Millipore Milli-Q system, resistivity: 18.2 M Ω cm at 25 °C) was used to prepare all solutions.

Antibiotic-resistant bacterial strains employed to contaminate the

synthetic urine matrix during the disinfection experiments were: 1) *P. aeruginosa* ATCC 9027 (CECT, Spain) harboring the *bla*_{OXA-50} gene, an oxacillinase β -lactam gene that confers resistance to ampicillin, ticarcillin, meropenem, etc.; 2) *S. aureus* ATCC 43300 (CECT, Spain) was selected for carrying the *mecA* gene which provides resistance to methicillin; 3) *K. pneumoniae* ATCC BAA-1705 (ThermoFisher Scientific, Spain) was a carbapenemase-producing carbapenem-resistant Enterobacteriaceae carrying the antibiotic-resistance *bla*_{KPC} gene.

2.2. Experimental procedure

Electrodisinfection experiments were carried out in a microfluidic flow-through reactor with an inter-electrode gap of 400 μ m, that minimizes ohmic drops [29]. It is based on a filter-press layout in which the effluent is fed perpendicularly to the electrodes as shown in Fig. S1. Photo-electrodisinfection experiments were carried out by coupling an UV germicidal lamp of 5 W (λ = 254 nm), located in the middle of the system. The anode material was supplied by Tianode® (India) and was a 3D mesh Mixed Metal Oxide (MMO, 70/30 IrO₂/Ta₂O₅). The cathode material, was handmade as can be found elsewhere [30] and was a 3D-titanium mesh with deposition of carbon black (CB) from Cabot Corporation (Vulcan® XC72) and PTFE (60 % wt. Teflon® in H₂O). Electrode dimensions of 9.5 \times 8 cm² and a surface area of 49.5 cm² were employed [31]. Each experiment was carried out in a bench-scale experimental set-up and conducted in triplicate under galvanostatic conditions. A Delta Electronika ES030–10 power supply (0–30 V, 0–10A) provided the electric current. The effluent with an initial volume of 2 dm³ was recirculated at a constant flow rate of 160 dm³ h⁻¹. A current density of 50 A m⁻² was selected considering previous studies were a higher efficiency in the generation of disinfectant species (mainly chloramine and hypochlorite) for the microfluidic-flow through reactor [32,33].

Hospital urine was simulated by employing a synthetic human urine electrolyte that intensified with one of the three different ARB tested (*P. aeruginosa*, *S. aureus* or *K. pneumoniae*) at an initial concentration of 10⁷ CFU mL⁻¹. The composition of the synthetic urine employed has been previously reported elsewhere [34]. Bacterial strains were cultured at 37 °C for 24 h in Tryptone Soy Agar plates (Scharlab S.L.) before being resuspended into the synthetic urine.

All experiments were conducted in triplicate, and the results were expressed as the mean values since the standard deviation in biological and chemical analyses was below 5 %.

2.3. Biological analyses

2.3.1. Bacterial concentration

The concentration of *P. aeruginosa*, *S. aureus* and *K. pneumoniae* was determined using the μ -Trac® 4200 system. This is an analytical equipment based on an indirect impedance method. It records changes in the standard impedance signal in an AC field due to the breakdown of nutrients (microbial metabolisms of ARB) [35,36]. Impedance values were related to ARB concentrations in CFU mL⁻¹ through initial calibrations of each bacterium by plate count. Nutrient media employed for ARB counting contained calcium chloride dihydrate for the determination of total viable count medium (BiMedia 001B) supplied by SY-LAB.

2.3.2. DNA analysis

Samples were previously centrifuged as described in the literature and subsequently, DNA was extracted using a commercial Urine DNA Isolation Kit (Norgen Biotek) [37,38]. The DNA concentration was determined for the initial (DNA_{initial}, 0 min) and final (DNA_{final}, 180 min) samples by measuring the absorbance at 260 nm in a spectrophotometer (Biochrom Libra S70) [39]. Eq. (1) is used to calculate the removal of DNA to study the effect of the disinfection technologies tested.

$$\text{Log removal of DNA} = \log_{10} \left(\frac{\text{DNA}_{\text{initial}}}{\text{DNA}_{\text{final}}} \right) \quad (1)$$

2.3.3. ARGs analysis

Primers for *bla*_{OXA-50} gene (PowerUp™ SYBR™ Green Master Mix) were designed based on a previous study by Jaafar et al. [40], and ordered for its preparation in Thermo Fischer Scientific, Spain. The forward and reverse primers were chosen for *bla*_{OXA-50} gene quantification were 5'-GAAAGGCACCTTCGTCCTCTAC-3' and 5'-CAGAAAGTGGGTCTGTTCATC-3', respectively. Commercial primers and probes used for *mecA* gene (TaqMan® Gene Expression Assays (FAM)) were supplied by Thermo Fischer Scientific, Spain. Finally, *bla*_{TEM} gene primers (PowerUp™ SYBR™ Green Master Mix) were designed based on a previous study by Bibbal et al. [41], and ordered for its preparation (Thermo Fischer Scientific, Spain). For the quantification of *bla*_{TEM} gene, forward (5'-TTCCTGTTTTGCTCACCCAG-3') and reverse (5'-CTCAAGGATCTTACCGCTGTTG-3') primers, were chosen.

The ARGs (*bla*_{OXA-50}, *mecA* and *bla*_{KPC}) quantification were developed by amplification using a QuantStudio 5 Real-Time PCR System (Thermo Fischer Scientific, Spain). The qPCR amplification for *bla*_{OXA-50} gene was developed at 50 °C for 2 min and 95 °C for 2 min, followed by 50 cycles of 95 °C for 15 s, 56 °C for 15 s and 72 °C for 60 s. A 20-μL reaction mixture containing 10 μL of PowerUp™ SYBR™ Green Master Mix and 1 μL of each primer, 50 ng of extracted DNA and ultrapure water to 20 μL were used for the amplification of *bla*_{OXA-50} gene. The qPCR amplification for *mecA* gene was carried out at 50 °C for 2 min and 95 °C for 2 min, followed by 40 cycles of 95 °C for 1 s and 61 °C for 20 s. A 20-μL reaction mixture containing 10 μL of TaqMan™ Fast Advanced Master Mix, 1 μL of TaqMan® Gene Expression Assays (FAM), 50 ng of extracted DNA and ultrapure water to 20 μL were used for the amplification of *mecA* gene. Finally, the amplification of *bla*_{KPC} gene was performed at 50 °C for 2 min and 95 °C for 2 min followed by 40 cycles of 95 °C for 1 s and 61 °C for 20 s. A 20-μL reaction mixture containing 10 μL of PowerUp™ SYBR™ Green Master Mix and 1 μL of each primer, 50 ng of extracted DNA and ultrapure water to 20 μL were used for the amplification of *bla*_{KPC} gene. The qPCR assays were measured in triplicate.

The qPCR system determines the number of amplification cycles required to reach the exponential growth phase, usually named cycle threshold (C_T). Fig. 1 plots C_T vs. bacterial log reduction for the three ARGs studied. Furthermore, Eq. (2) is proposed to correlate C_T values with the logarithmic removal of ARGs. During the experiments, ARGs concentrations in initial ($C_{T, \text{initial}}$, 0 min) and final ($C_{T, \text{final}}$, 180 min)

samples were determined and the Gradient_{standard curve} represent the slope (C_T /bacterial log reduction) of the calibration curves of Fig. 1.

$$\text{Log removal of ARGs} = \frac{C_{T, \text{final}} - C_{T, \text{initial}}}{\text{Gradient}_{\text{standard curve}}} \quad (2)$$

2.4. Chemical analyses

Hypochlorite anions were determined with an 888 Titrand system (Metrohm Hispania, Spain). Titration solution employed consisted of 0.001 M As₂O₃ in 2 M NaOH [42,43]. The DPD (N,N-diethyl-phenylenediamine) standard colorimetric method was employed to measure inorganic chloramines [44]. Hydrogen peroxide concentration was measured by a spectrophotometric method, which determines the concentration of the complex formed between H₂O₂ and Ti⁴⁺ [45]. The pH and conductivity were monitored using a Sension+ MM150 Portable Multi-Parameter Meter (HACH).

3. Results and discussion

Fig. 2 plots the occurrence of the most prevalent microorganism, which causes urinary tract infections (UTIs) in the University Hospital Complex of Albacete (Spain) within the period of 2014–2018. The study was carried out with 4453 urine samples that were positive for at least one pathogen. The urine samples belonged to patients hospitalized in the geriatrics, hematology, oncology and medical and surgical intensive care wards. The pathogens were grouped in the following three families: gram-negative bacteria (blue colour), gram-positive bacteria (orange colour) or yeasts (green colour).

As can be observed, most of the microorganisms causing UTIs belong to the gram-negative bacteria group, representing 62.78 % of the total microorganisms analysed. Indeed, the main bacteria causing UTIs were *Escherichia coli* (*E. coli*) with a presence percentage of 37.05 %, follows by *K. pneumoniae* and *P. aeruginosa* with 8.46 and 5.16 %, respectively. It is noticeable that antibiotic-resistant strains of *K. pneumoniae* and *P. aeruginosa* have been recently reported for the serious threat involved in sanitary environments [4,46]. Specifically, these ARB present a poor response to antibiotic treatments and their outbreak often causes life-threatening nosocomial infections with a plethora of symptoms such as severe pneumonia, lung infections, sepsis or multiorgan failure [5,6].

Furthermore, gram-positive bacteria and yeasts were also present in 21.70 and 15.51 % of the total microorganisms analysed, respectively. *Enterococcus faecalis* (*E. faecalis*), *Enterococcus faecium* (*E. faecium*), *Staphylococcus epidermidis* (*S. epidermidis*) and *S. aureus* were the main gram-positive bacteria causing UTIs with a prevalence of 50.41, 14.64, 7.32 and 5.95 %, respectively. It is of special relevance the infections caused by antibiotic-resistant *S. aureus* since it is a common human pathogenic bacteria with a wide range of virulence factors and high adaptability and tenacity that can result in infectious diseases such as skin infections, endocarditis, bacteremia or lethal pneumonia among others [47,48]. On the other hand, the genus *Candida* mainly cope the yeasts analysed in the study. In the last years, drug resistance in yeasts is becoming an emerging and threatening scenario due to the lack of effective treatment alternatives [49]. However, the prevalence of antibiotic resistance strains in gram-negative and gram-positive bacteria over yeasts can be clearly depicted from the report on antibiotic resistance in the United States published by the U.S. Department of Health and Human Services [2].

In this context, antibiotic-resistant strains of *K. pneumoniae*, *P. aeruginosa* and *S. aureus* have been employed as target bacteria for the disinfection processes tested in the present work. To control the dissemination of ARB into the environment and to reduce potential horizontal transfer processes, it is of crucial importance the removal of deoxyribonucleic acid (DNA) and antibiotic resistance genes (ARGs) present in the antibiotic-resistant bacterial strains. The occurrence of the coexistence of several ARGs in a single bacterial strain is a factor that

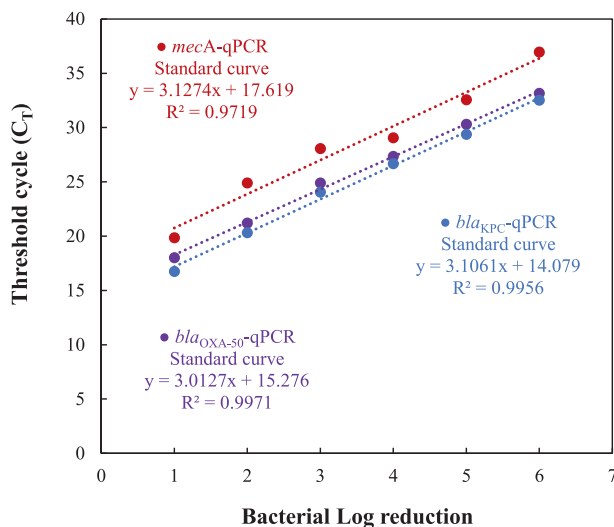


Fig. 1. Standard curves of the relationship between cycle threshold (C_T) and the concentration of *bla*_{KPC}, *mecA* and *bla*_{OXA-50} genes for qPCR.

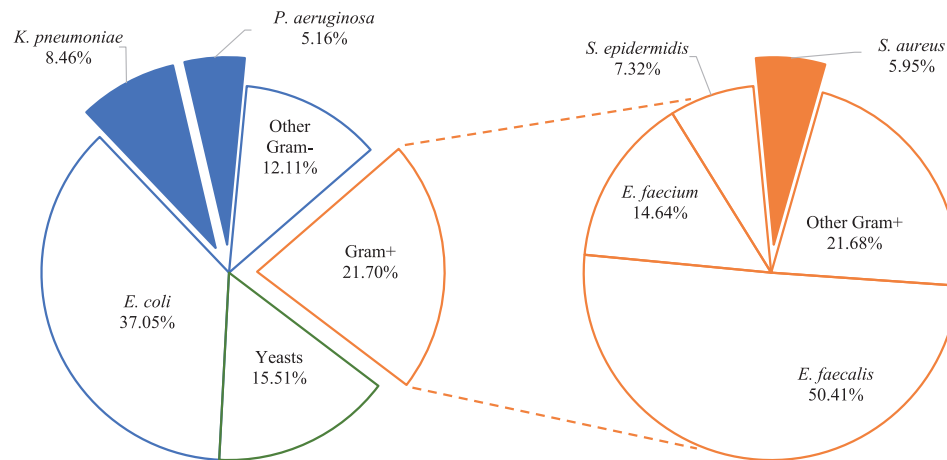


Fig. 2. Distribution of the main microorganisms present in hospital urines from patients suffering urinary tract infections at University Hospital Complex of Albacete within the period 2014–2018.

amplifies the danger posed by the bacterium. In this regard, to gain insight into the ARGs composition of the three ARB tested in this work, a search of the main genes responsible for carrying antibiotic resistance through different resistance mechanisms has been carried out in the *National Center for Biotechnology Information* (NCBI) database. During this search, the nucleotide sequence of the three ARB was continuously compared with the sequences of the ARGs tested and sequences with a homology percentage higher than 99 % were assigned to their resistance mechanism.

Table 1 summarized the ARGs present in *K. pneumoniae* ATCC BAA-1705, *P. aeruginosa* ATCC 9027 and *S. aureus* ATCC 43300, grouped based on the resistance mechanism to antibiotics. Among the major resistance mechanisms present in ARB are 1) limiting drug uptake: drugs that target the cell wall (mainly β -lactams and glycopeptides) enter the cell through porin channels in the outer membrane, 2) drug target modification: bacteria are able to modify the components that are targeted by drugs to enable resistance to those drugs, 3) drug inactivation: this mechanism can proceed by the degradation of the drug or by the transference of a chemical group to inactivate the drug, 4) drug efflux: bacteria that contain chromosomally encoded genes for efflux pumps have the capacity to rid drugs out of the cell, and many of these pumps

transport a large variety of compounds (multi-drug efflux pumps) [50–52].

In this work, *bla*_{KPC}, *bla*_{OXA-50} and *mecA* genes were selected as ARG models for *K. pneumoniae*, *P. aeruginosa* and *S. aureus*, respectively. The *K. pneumoniae* strains harboring the *bla*_{KPC} gene represent the most common cause of carbapenem resistance in *Enterobacteriaceae* [53]. Carbapenemases hydrolyze carbapenem antibiotics and other β -lactam antibiotics provide a high antibiotic resistance [54]. The *bla*_{OXA-50} gene is an oxacillinase β -lactam gene that confers a decreased susceptibility to antibiotics such as ampicillin, ticarcillin, moxalactam or meropenem [55]. Finally, the *mecA* gene encodes a low/affinity penicillin-binding protein (PBP 2A), which provides resistance to methicillin [56]. Likewise, the *mecA* gene is part of a mobile genetic element that may also provide resistance to non- β -lactam antibiotics through other contained genetic structures (Tn554, pUB110 or pT181) [57].

In this regard, Fig. 3a shows the evolution of ARB (*K. pneumoniae*, *P. aeruginosa*, *S. aureus*) as a function of the applied electric charge whereas Fig. 3b plots the performance of ARGs (*bla*_{KPC}, *bla*_{OXA-50} and *mecA* genes) and DNA, during the electrodisinfection and photo-electrodisinfection of synthetic hospital urines.

Results show that the electrodisinfection process achieved removal ratios higher than 4-logs by applying an electric charge of 0.423 Ah dm⁻³ (180 min). It is remarkable that the efficiency of the electrodisinfection process varied within a logarithmic order of magnitude among the target ARB tested. Specifically, log removals of 4.9, 5.8 and 7 (total disinfection) were achieved for *P. aeruginosa*, *S. aureus* and *K. pneumoniae*, respectively. However, results also show that slightly log increments of 0.71, 0.18 and 0.19 were obtained during the electrodisinfection experiments for *bla*_{KPC}, *bla*_{OXA-50} and *mecA* genes, respectively. Indeed, the logarithmic increments of ARGs seem to be promoted with the higher removal efficiency of each ARB tested (*bla*_{KPC} (*K. pneumoniae*) > *mecA* (*S. aureus*) > *bla*_{OXA-50} (*P. aeruginosa*)). In addition, an almost negligible removal of DNA was observed for every electrodisinfection experiment conducted.

On the other hand, the coupling of UV light with the electrodisinfection process significantly enhance the disinfection efficiency of the process, reaching the complete disinfection regardless of the target ARB tested. The removal of *P. aeruginosa* is observed to be slightly more efficient than the removal of *K. pneumoniae* or *S. aureus* since the complete disinfection is attained at 0.278 Ah dm⁻³ (120 min). Additionally, logarithmic removals of DNA of 0.172, 0.239 and 0.153 were attained during the photo-electrodisinfection experiments for the synthetic hospital urines infected with *K. pneumoniae*, *P. aeruginosa* and *S. aureus*, respectively. Likewise, results also showed that log removals of 0.82, 3.70 and 2.25 were obtained during the photo-electrodisinfection

Table 1

Resistance mechanisms attributed to the presence of ARGs in the bacterial strains employed.

ARB strain	Resistance mechanisms of ARGs			
	Limiting drug uptake (β -lactams)	Drug target modification	Drug inactivation	Drug efflux
<i>K. pneumoniae</i> ATCC BAA-1705	<i>bla</i> _{TEM} <i>bla</i> _{SHV} <i>bla</i> _{KPC}	<i>gyrA</i> <i>gyrB</i> <i>parE</i> <i>parC</i>	<i>aac</i> <i>aada</i>	<i>acrA</i> <i>acrR</i>
<i>P. aeruginosa</i> ATCC 9027	<i>bla</i> _{ACT} <i>bla</i> _{OXA-50}	<i>gyrA</i> <i>gyrB</i>	<i>antA</i> (1)	<i>mexA</i> <i>mexB</i> <i>OprM</i> <i>OprD</i> <i>acrA</i> <i>acrB</i> (1) <i>norA</i>
<i>S. aureus</i> ATCC 43300	<i>bla</i> _{ARLR} <i>bla</i> _{ARLS}	<i>tet</i> (38) <i>mgrA</i> <i>gyrA</i>	<i>mepA</i> <i>mepB</i> <i>mepR</i> <i>fabI</i> <i>mecA</i> <i>mec1</i> <i>mecR1</i> <i>ermA</i>	

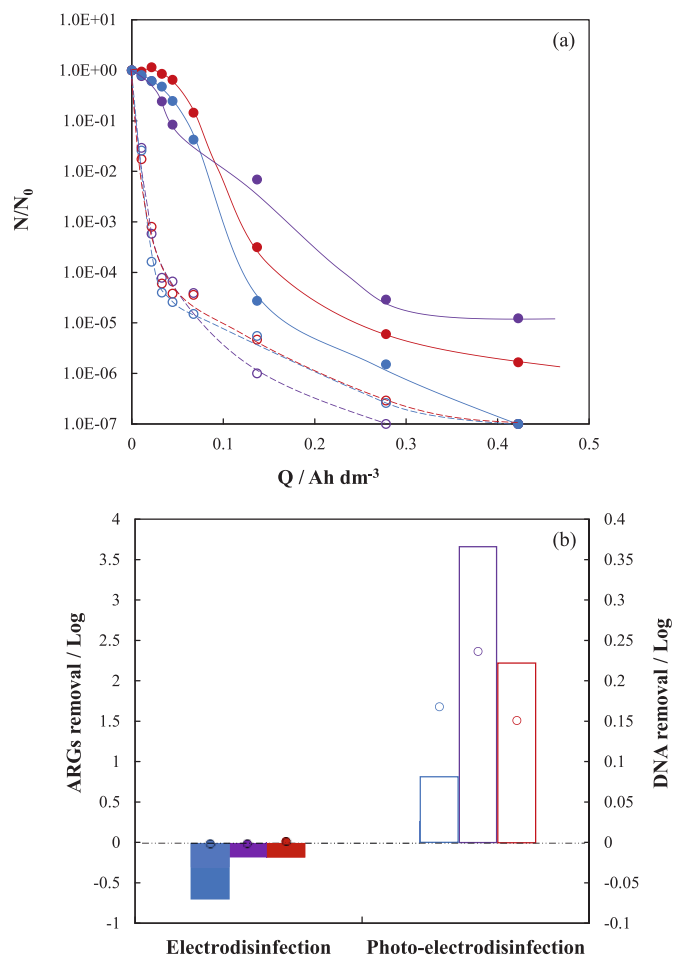


Fig. 3. Evolution of ARB concentration with the applied electric charge (Fig. 3a) and performance of ARGs (bars) and DNA (points) (Fig. 3b), during the disinfection of hospital urines using a microfluidic flow-through reactor at 50 A m⁻². Electrochemical technology: electrolysis (full symbols); photo-electrolysis (empty symbols). ARB, ARGs tested: *K. pneumoniae*, bla_{KPC} (blue colour); *P. aeruginosa*, bla_{OXA-50} (purple colour); *S. aureus*, mecA (red colour). (For interpretation of the references to colour in this figure legend, the reader is referred to the web version of this article.)

experiments for bla_{KPC}, bla_{OXA-50} and mecA genes, respectively. In fact, the more efficient the removal of ARB, the higher the removal of ARGs.

The performance of ARB, ARGs and DNA of each strain tested may be related to the disinfectant species electrogenerated during the electrodisinfection process and/or even the possible photo-activation of these disinfectant species during the photo-electrodisinfection process. To shed light on it, the generation of the different expected disinfectant species were followed during both disinfection processes. Firstly, the use of a titanium cathode with a carbon black/polytetrafluoroethylene (CB/PTFE) mixture should promote the generation of hydrogen peroxide by oxygen reduction (Reaction 1) [58–60]. The concentration of hydrogen peroxide was monitored during the electrodisinfection and photo-electrodisinfection processes (data not shown), although negligible measurements were obtained for every test. This fact does not mean a null electrogeneration of hydrogen peroxide but a fast decomposition which could be related with parasitic reactions such as its self-decomposition (Reaction 2), its oxidation in the anode surface to produce oxygen (Reaction 3), its reduction in the cathode surface to water (Reaction 4) or its reaction with organic compounds and/or bacteria present in urine media [29,61,62]. Likewise, hydrogen peroxide may be activated with UV light to promote the generation of hydroxyl radicals (Reaction 5) during the photo-electrodisinfection process [12]. In fact,

Moratalla et al. reported the performance on the electrogeneration of hydrogen peroxide using a microfluidic flow-through reactor with a MMO anode and a CB/PTFE cathode working at 50 A m⁻² [30]. The treatment of urines in the absence of their organic compounds led to maximum accumulations of 24.99 mg H₂O₂ dm⁻³ (0.8 Ah dm⁻³) working at atmospheric pressure.



Similarly, the evolution of chlorine derived disinfectant species as hypochlorite was also monitored. In our previous works, the evolution of hypochlorite was studied during the electrolysis of urines in the absence of their organic compounds using a microfluidic flow-through reactor with a MMO anode and a stainless-steel cathode at 50 A m⁻². This test proved the increase in the generation of hypochlorite as a final product, reaching maximum concentrations around 1.8 mmol dm⁻³ Cl⁻ClO⁻ (0.423 Ah dm⁻³) [32]. However, no significant concentrations of hypochlorite were detected in the present work since this is a very reactive species that i) can react to degrade organic compounds and to kill bacteria from urine, ii) can promote to other chlorine species in a higher oxidation state such as chlorate and/or perchlorate, iii) can chemically react with ammonium ions ([NH₄⁺]_{urine} = 22.72 mg dm⁻³) to produce inorganic chloramines (Reactions 6–8) or even iv) can be activated with UV light to produce chlorine radicals (Reaction 9) [10,63]. On the one hand, the formation of hazardous chloro-species as chlorates and perchlorates was avoided due to the high complexity of urine media [64]. On the other hand, chloramines show higher stability than hypochlorite, being easier to measure as they maintain an acceptable residual concentration in solution over time [65]. Herein, the evolution of the concentration of total chloramines is shown in Fig. 4 as a function of the applied electric charge during the electrodisinfection and photo-electrodisinfection of hospital urines infected with

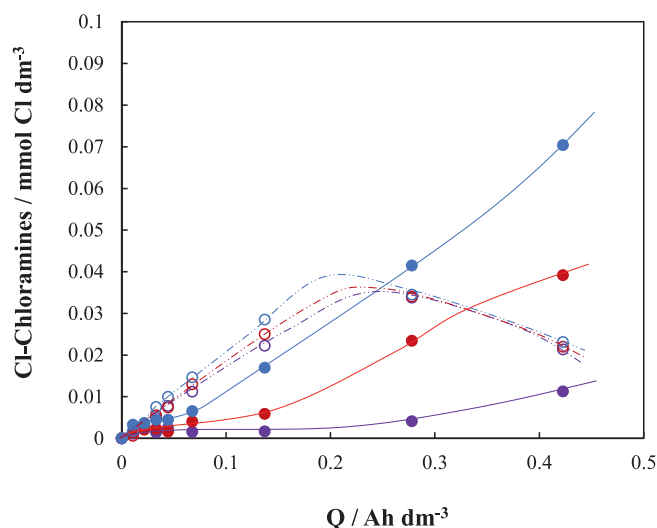


Fig. 4. Evolution of total inorganic chloramines with the applied electric charge during the disinfection of hospital urines using a microfluidic flow-through reactor at 50 A m⁻². Electrochemical technology: electrolysis (full symbols); photo-electrolysis (empty symbols). ARB, ARGs tested: *K. pneumoniae*, bla_{KPC} (blue colour); *P. aeruginosa*, bla_{OXA-50} (purple colour); *S. aureus*, mecA (red colour). (For interpretation of the references to colour in this figure legend, the reader is referred to the web version of this article.)

K. pneumoniae, *P. aeruginosa* or *S. aureus*. Total inorganic chloramines correspond to the sum of monochloramine (NH_2Cl), dichloramine (NHCl_2) and trichloramine (NCl_3) which each prevalence depends on the pH of the bulk solution [66]. NHCl_2 followed by NH_2Cl should be mainly promoted since pH values ranged from 5 to 6 during these disinfection experiments.



As can be observed, different behavior in the evolution of chloramines was observed during the electrodisinfection and the photo-electrodisinfection tests. The concentration of chloramines continuously increased with the applied electric charge during electrodisinfection tests with a significant influence on the target ARB. Specifically, maximum values of 0.070, 0.039 and 0.011 mmol $\text{Cl-NH}_x\text{Cl}_y \text{ dm}^{-3}$ were obtained at the end of each test (0.423 Ah dm^{-3}) for the urine matrices infected with *P. aeruginosa*, *S. aureus* and *K. pneumoniae*, respectively. Opposite to that, the chloramine's generation showed a negligible influence of the target ARB studied during the photo-electrodisinfection tests. Initially, a greater accumulation of chloramines was generated until reaching maximum values around 0.035 mmol $\text{Cl-NH}_x\text{Cl}_y \text{ dm}^{-3}$ at 0.278 Ah dm^{-3} . After that, the concentration of chloramines started to decrease toward 0.020 mmol $\text{Cl-NH}_x\text{Cl}_y \text{ dm}^{-3}$ at 0.423 Ah dm^{-3} , showing a typical profile of an intermediate compound.

In this context, the competitiveness of hypochlorite to attack bacteria or to degrade organic urine compounds for the release of nitrogen species could be helpful to explain the different chloramine profiles are observed in Fig. 4. It is noticeable that hypochlorite exhibits a higher bactericidal effect in comparison with chloramines because chloramines require longer exposure times to inactive microorganisms [67]. Additionally, it is known that urine contains not only inorganic nitrogen from 17.67 mg dm^{-3} $\text{N-(NH}_4)_2\text{HPO}_4$, but also organic nitrogen from $\text{N-CH}_4\text{N}_2\text{O}$ (urea), $\text{N-C}_4\text{H}_7\text{N}_3\text{O}$ (creatinine) and $\text{N-C}_5\text{H}_4\text{N}_4\text{O}_3$ (uric acid) in concentrations of 1554.00, 61.88 and 16.66 mg dm^{-3} , respectively [67]. The soft operational conditions used for disinfection tests (50 A m^{-2}) lead to a smooth degradation of these organics as summarized in Table 2.

The organic compound in a higher concentration (urea) exhibited the lowest removal percentages of 5.75, 4.52 and 2.66 % compared with creatinine (5.89, 4.60 and 2.37 %) and uric acid (86.72, 81.77 and 78.57 %), obtained during electrodisinfection tests of urines containing *K. pneumoniae*, *S. aureus* and *P. aeruginosa*, respectively. In this regard, the degradation of organic compounds during electrodisinfection tests

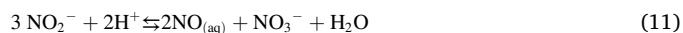
seems to be influenced by the presence of the different ARB in the urine matrix. In fact, the higher the removal of ARB / ARGs plotted in Fig. 3 the higher the degradation of organics from urine shown in Table 2, due to the loss of competitiveness of hypochlorite in attacking ARB instead of degrading organics. Furthermore, as expected, the highest removal rates of organic compounds were observed during photo-electrodisinfection tests [68–70]. A mean increment in the degradation percentage of 0.30, 2.17 and 3.00 % were obtained for urea, creatinine and uric acid, respectively, compared with the ones obtained for the electrodisinfection processes.

The degradation of urea, creatinine and uric acid leads to the release of nitrogen into solution. Herein, Fig. 5 shows the evolution of nitrogen species as nitrite (Fig. 5a), nitrate (Fig. 5b) and ammonium ions (Fig. 5c) with the applied electric charge during the disinfection of hospital urines.

The degradation of N-N_{org} is known to firstly produce the highly reactive N-NO_2^- (Reaction 10) as shown in Fig. 5a [71]. As can be observed, it can be appreciated an initial zone with a null concentration of N-NO_2^- until 0.05 Ah dm^{-3} , from which N-NO_2^- concentration increased gradually for electrodisinfection tests up to around 0.13 mmol $\text{N-NO}_2^- \text{ dm}^{-3}$ regardless of the target ARB studied.



Nitrite may be considered a key intermediate nitrogen specie because it may be oxidized or reduced by many chemicals due to its intermediate oxidation state (+3) [72]. Nitrite has been reported to follow a disproportionation reaction in acidic media to mainly produce nitrate and nitric oxide, and it may be also oxidized into nitrates due to the atmospheric oxygen moved into the aqueous media (Reactions 11–12) [73]. The nitrate profiles observed in Fig. 4b shows that N-NO_3^- concentration continuously increases during the electrodisinfection tests. Specifically, maximum accumulations in the bulk solution of 0.109, 0.080 and 0.069 mmol $\text{N-NO}_3^- \text{ dm}^{-3}$ were monitored at 0.423 Ah dm^{-3} for urines containing *K. pneumoniae*, *S. aureus* and *P. aeruginosa*, respectively. In fact, this evolution agrees the maximum accumulations observed for chloramines during electrodisinfection tests showed in Fig. 4, bearing in mind that nitrates are known to always evolve to ammonium ions as the final electrochemical reduction products (Reactions 13–14) [32,71,73]. The higher the accumulation of chloramines in the bulk solution the higher the efficiency on the removal of ARB (Fig. 3a) since hypochlorite would tend to degrade organics. In this regard, final concentrations around 1.70 mmol $\text{N-NH}_4^+ \text{ dm}^{-3}$ were observed for each electrodisinfection test in Fig. 5c since the concentrations of ammonium ions monitored were not referred to the total concentration generated but those that have not reacted with other compounds, thus accumulating in the bulk solution.



A similar performance of nitrogen species may be described for the photo-electrodisinfection tests although it should be highlighted the higher nitrogen release observed due to the higher degradation percentages of organics from urine. As can be observed, the accumulation of nitrogen species at 0.423 Ah dm^{-3} ranges from 0.23 to 0.33 mmol $\text{N-NO}_2^- \text{ dm}^{-3}$, from 0.12 to 0.13 mmol $\text{N-NO}_3^- \text{ dm}^{-3}$ and from 1.75 to 1.88 mmol $\text{N-NH}_4^+ \text{ dm}^{-3}$ during photo-electrodisinfection tests. Additionally, UV light promotes the formation of nitrogen radicals from nitrite or nitrate (Reactions 15–16) which may contribute to enhance the efficiency on the removal of target ARB during photo-electrodisinfection [74].

Table 2

Degradation percentage of organic compounds contained in hospital urines at 50 A m^{-2} .

Technology	Target ARB / ARGs	Degradation percentage (%)		
		Urea	Creatinine	Uric acid
Electrodisinfection	<i>K. pneumoniae</i> / <i>bla</i> _{KPC}	5.75	5.89	86.72
	<i>P. aeruginosa</i> / <i>bla</i> _{OXA-50}	2.66	2.37	78.57
	<i>S. aureus</i> / <i>mecA</i>	4.52	4.60	81.77
	<i>K. pneumoniae</i> / <i>bla</i> _{KPC}	6.12	7.48	86.37
Photo-electrodisinfection	<i>P. aeruginosa</i> / <i>bla</i> _{OXA-50}	2.91	4.84	84.13
	<i>S. aureus</i> / <i>mecA</i>	4.81	7.06	85.55

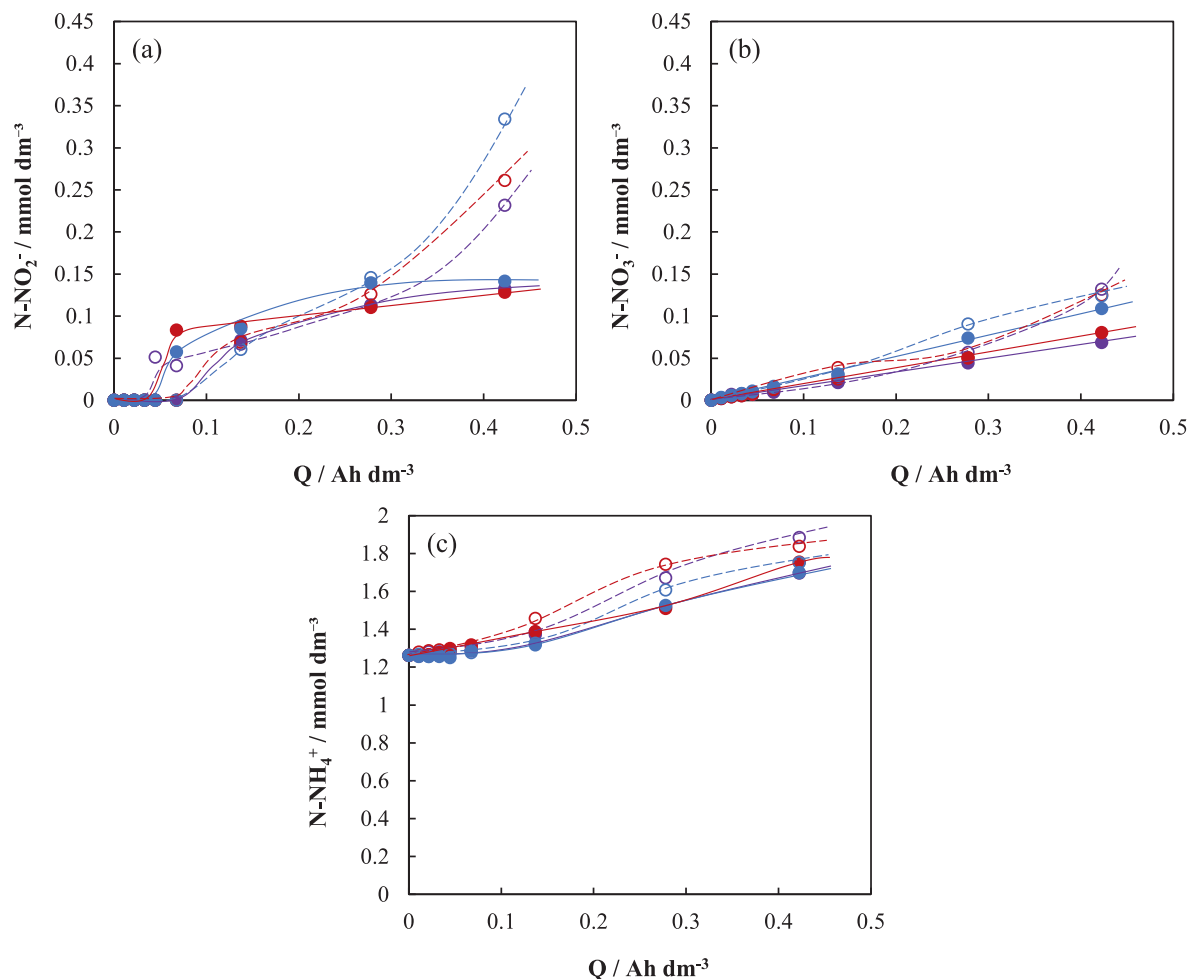


Fig. 5. Evolution of nitrogen species as nitrite (a), nitrate (b) and ammonium ions (c) with the applied electric charge during the disinfection of hospital urines using a microfluidic flow-through reactor at 50 A m^{-2} . Electrochemical technology: electrolysis (full symbols); photo-electrolysis (empty symbols). ARB, ARGs tested: *K. pneumoniae*, *bla_{KPC}* (blue colour); *P. aeruginosa*, *bla_{OXA-50}* (purple colour); *S. aureus*, *mecA* (red colour). (For interpretation of the references to colour in this figure legend, the reader is referred to the web version of this article.)



Despite N-NH_4^+ concentration is observed to continuously increase with the applied electric charge during the photo-electrodisinfection tests, the concentration of chloramines started to decrease after 0.278 Ah dm^{-3} (Fig. 4) when the removal of ARB was up to 6-logs (Fig. 3a). This fact could be explained considering the competitiveness of UV light between killing ARB and degrading formed chloramines. The depletion of chloramines under UV light exposure at 254 nm follows photolysis rate constants of $9.0 \pm 0.7 \times 10^{-4}$, $9.1 \pm 0.7 \times 10^{-4}$ and $4.5 \pm 0.2 \times 10^{-3} \text{ cm}^2 \text{ mJ}^{-1}$ for NH_2Cl , NHCl_2 and NCl_3 , respectively [75]. In addition, it has been reported the formation of chlorine and nitrogen radicals from the fracture of the N-Cl bonds in NH_2Cl and NHCl_2 as a consequence of the UV light irradiation (Reactions 17–18) [76,77]. It is also remarkable that the formation of chlorine and nitrogen radicals can contribute not only to the bacteria killing but also to their ARGs depletion, which could explain the improvement in the disinfection efficiencies of the photo-electrodisinfection process in comparison with electrodisinfection process as shown in Fig. 3. Finally, Fig. 6 illustrates the disinfection mechanisms that have been previously described during the electrodisinfection and photo-electrodisinfection processes.



4. Conclusions

The antibiotic-resistant strains of *K. pneumoniae*, *P. aeruginosa* and *S. aureus* were selected as target ARB, considering their prevalence to cause UTIs in patients from the University Hospital Complex of Albacete (Spain). The disposal of these untreated hospital urines would lead to outcome a significant sanitary and environmental risk. A microfluidic flow-through reactor (MMO anode, CB/PTFE cathode) was used for the electrochemical treatment of simulated hospital urines at 50 A m^{-2} , attaining ARB removals of 4.9, 5.8 and 7 logs (total disinfection) at 0.423 Ah dm^{-3} for *P. aeruginosa*, *S. aureus* and *K. pneumoniae*, respectively. The killing of ARB takes place due to the formation of hypochlorite, although it is not only a powerful disinfectant but also a powerful oxidant. Thus, hypochlorite seems to develop competitive reactions between killing ARB and degrading organics from urine, which leads to release inorganic nitrogen species as nitrates and then, promoting the formation of chloramines. Additionally, the coupling of UV light to the electrodisinfection process significantly enhance the disinfection efficiency, reaching the complete disinfection for each ARB tested. Furthermore, log removals of 3.70, 2.25 and 0.82 were also attained for *bla_{OXA-50}*, *mecA* and *bla_{KPC}* genes, respectively. These outcomes reveal the promotion of chlorine and even nitrogen radicals

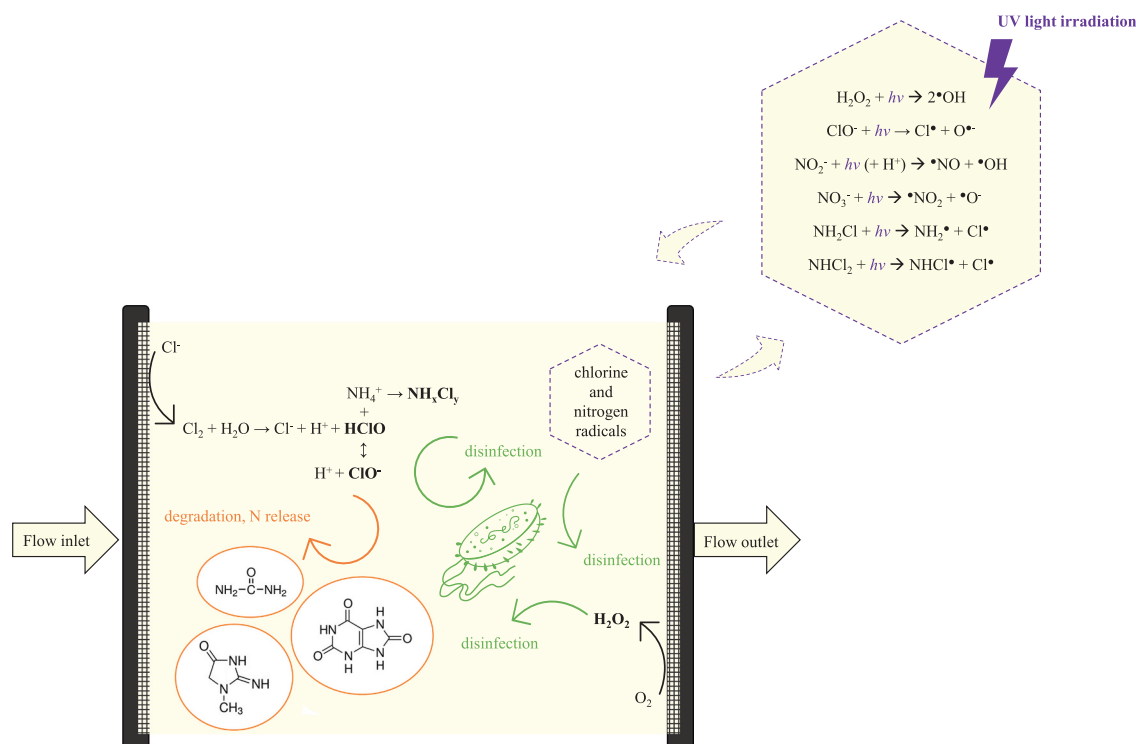


Fig. 6. Illustration of the disinfection mechanisms of bacteria.

which contribute to enhance the disinfection efficiency of the target ARB / ARGs in urine.”

Supplementary data to this article can be found online at <https://doi.org/10.1016/j.jwpe.2022.103035>.

Declaration of competing interest

The authors declare that they have no known competing financial interests or personal relationships that could have appeared to influence the work reported in this paper.

Data availability

No data was used for the research described in the article.

Acknowledgments

Financial support from Ministry of Science and Innovation through the project PID2019-110904RB-I00 is gratefully acknowledged.

References

- [1] A. Cassini, L.D. Högberg, D. Plachouras, A. Quattrocchi, A. Hoxha, G.S. Simonsen, M. Colomb-Cotinat, M.E. Kretzschmar, B. Devleeschauwer, M. Cecchini, Attributable deaths and disability-adjusted life-years caused by infections with antibiotic-resistant bacteria in the EU and the European Economic Area in 2015: a population-level modelling analysis, *Lancet Infect. Dis.* 19 (2019) 56–66.
- [2] CDC, Antibiotic Resistance Threats in the United States, 2019, U.S. Department of Health and Human Services, CDC, Atlanta, GA, 2019.
- [3] M.G. Lorenz, W. Wackernagel, Bacterial gene transfer by natural genetic transformation in the environment, *Microbiol. Rev.* 58 (1994) 563–602.
- [4] D.M.P. De Oliveira, B.M. Forde, T.J. Kidd, P.N.A. Harris, M.A. Schembri, S. A. Beatson, D.L. Paterson, M.J. Walker, Antimicrobial resistance in ESKAPE pathogens, *Clin. Microbiol. Rev.* 33 (2020).
- [5] D. Gu, N. Dong, Z. Zheng, D. Lin, M. Huang, L. Wang, E.W.C. Chan, L. Shu, J. Yu, R. Zhang, S. Chen, A fatal outbreak of ST11 carbapenem-resistant hypervirulent *Klebsiella pneumoniae* in a Chinese hospital: a molecular epidemiological study, *Lancet Infect. Dis.* 18 (2018) 37–46.
- [6] M.S. Mulani, E.E. Kamble, S.N. Kumkar, M.S. Tawre, K.R. Pardesi, Emerging strategies to combat ESKAPE pathogens in the era of antimicrobial resistance: a review, *Front. Microbiol.* 10 (2019).
- [7] J. Lienert, M. Koller, J. Konrad, C.S. McArdell, N. Schuwirth, Multiple-criteria Decision Analysis Reveals High Stakeholder Preference to Remove Pharmaceuticals From Hospital Wastewater, ACS Publications, 2011.
- [8] J. Singla, V.K. Sangal, A. Singh, A. Verma, Application of mixed metal oxide anode for the electro-oxidation/disinfection of synthetic urine: potential of harnessing molecular hydrogen generation, *J. Environ. Manag.* 255 (2020).
- [9] S. Dbira, N. Bensalah, M.I. Ahmad, A. Bedoui, Electrochemical oxidation/disinfection of urine wastewaters with different anode materials, *Materials* 12 (2019) 1254.
- [10] S. Cotillas, E. Lacasa, C. Sáez, P. Cañizares, M.A. Rodrigo, Disinfection of urine by conductive-diamond electrochemical oxidation, *Appl. Catal. B Environ.* 229 (2018) 63–70.
- [11] A.S. Raut, C.B. Parker, E.J.D. Klem, B.R. Stoner, M.A. Deshusses, J.T. Glass, Reduction in energy for electrochemical disinfection of *E. Coli* in urine simulant, *J. Appl. Electrochem.* 49 (2019) 443–453.
- [12] M. Herraiz-Carboné, S. Cotillas, E. Lacasa, C. Sainz de Baranda, E. Riquelme, P. Cañizares, M.A. Rodrigo, C. Sáez, A review on disinfection technologies for controlling the antibiotic resistance spread, *Sci. Total Environ.* 797 (2021).
- [13] Y.-H. Wu, Y.-H. Wang, S. Xue, Z. Chen, L.-W. Luo, Y. Bai, X. Tong, H.-Y. Hu, Increased risks of antibiotic resistant genes (ARGs) induced by chlorine disinfection in the reverse osmosis system for potable reuse of reclaimed water, *Sci. Total Environ.* 815 (2022), 152860.
- [14] M. Jin, L. Liu, D.-N. Wang, D. Yang, W.-L. Liu, J. Yin, Z.-W. Yang, H.-R. Wang, Z.-G. Qiu, Z.-Q. Shen, D.-Y. Shi, H.-B. Li, J.-H. Guo, J.-W. Li, Chlorine disinfection promotes the exchange of antibiotic resistance genes across bacterial genera by natural transformation, *ISME J.* 14 (2020) 1847–1856.
- [15] G. Kampf, Biocidal agents used for disinfection can enhance antibiotic resistance in gram-negative species, *Antibiotics (Basel)* 7 (2018) 110.
- [16] C.M. Zhang, L.M. Xu, X.C. Wang, K. Zhuang, Q.Q. Liu, Effects of ultraviolet disinfection on antibiotic-resistant *Escherichia coli* from wastewater: inactivation, antibiotic resistance profiles and antibiotic resistance genes, *J. Appl. Microbiol.* 123 (2017) 295–306.
- [17] G. Wen, Q. Wan, X. Deng, R. Cao, X. Xu, Z. Chen, J. Wang, T. Huang, Reactivation of fungal spores in water following UV disinfection: effect of temperature, dark delay, and real water matrices, *Chemosphere* 237 (2019), 124490.
- [18] O. Baaloudj, I. Assadi, N. Nasrallah, A. El Jery, L. Khezami, A.A. Assadi, Simultaneous removal of antibiotics and inactivation of antibiotic-resistant bacteria by photocatalysis: a review, *J. Water Process Eng.* 42 (2021), 102089.
- [19] D. Venieri, I. Gounaki, M. Bikouvaraki, V. Binas, A. Zachopoulos, G. Kiriakidis, D. Mantzavinos, Solar photocatalysis as disinfection technique: inactivation of *Klebsiella pneumoniae* in sewage and investigation of changes in antibiotic resistance profile, *J. Environ. Manag.* 195 (2017) 140–147.
- [20] S.K. Ray, D. Dhakal, C. Regmi, T. Yamaguchi, S.W. Lee, Inactivation of *Staphylococcus aureus* in visible light by morphology tuned α -NiMoO₄, *J. Photochem. Photobiol. A Chem.* 350 (2018) 59–68.

- [21] I. Sirés, E. Brillas, M.A. Oturan, M.A. Rodrigo, M. Panizza, Electrochemical advanced oxidation processes: today and tomorrow. A review, *Environ. Sci. Pollut. Res.* 21 (2014) 8336–8367.
- [22] R. Dewil, D. Mantzavinos, I. Poullos, M.A. Rodrigo, New perspectives for advanced oxidation processes, *J. Environ. Manag.* 195 (2017) 93–99.
- [23] Y. Tu, W. Tang, L. Yu, Z. Liu, Y. Liu, H. Xia, H. Zhang, S. Chen, J. Wu, X. Cui, J. Zhang, F. Wang, Y. Hu, D. Deng, Inactivating SARS-CoV-2 by electrochemical oxidation, *Sci. Bull. (Beijing)* 66 (2021) 720–726.
- [24] H. Fang, Y. Liu, P. Qiu, H.-L. Song, T. Liu, J. Guo, S. Zhang, Simultaneous removal of antibiotic resistant bacteria and antibiotic resistance genes by molybdenum carbide assisted electrochemical disinfection, *J. Hazard. Mater.* 432 (2022), 128733.
- [25] C. Zhang, X. Zhao, C. Wang, I. Hakizimana, J.C. Crittenden, A.A. Laghari, Electrochemical flow-through disinfection reduces antibiotic resistance genes and horizontal transfer risk across bacterial species, *Water Res.* 212 (2022), 118090.
- [26] Y. Ahmed, F. Zhong, Z. Yuan, J. Guo, Simultaneous removal of antibiotic resistant bacteria, antibiotic resistance genes, and micropollutants by a modified photo-Fenton process, *Water Res.* 197 (2021).
- [27] Y. Yang, K. Wan, Z. Yang, D. Li, G. Li, S. Zhang, L. Wang, X. Yu, Inactivation of antibiotic resistant *Escherichia coli* and degradation of its resistance genes by glow discharge plasma in an aqueous solution, *Chemosphere* 252 (2020).
- [28] L. Zhang, H. Jin, H. Ma, K. Gregory, Z. Qi, C. Wang, W. Wu, D. Cang, Z. Li, Oxidative damage of antibiotic resistant *E. Coli* and gene in a novel sulfidated micron zero-valent activated persulfate system, *Chem. Eng. J.* 381 (2020), 122787.
- [29] J.F. Pérez, J. Llanos, C. Sáez, C. López, P. Cañizares, M.A. Rodrigo, Towards the scale up of a pressurized-jet microfluidic flow-through reactor for cost-effective electro-generation of H₂O₂, *J. Clean. Prod.* 211 (2019) 1259–1267.
- [30] Á. Moratalla, D.M. Araújo, G.O.M.A. Moura, E. Lacasa, P. Cañizares, M.A. Rodrigo, C. Sáez, Pressurized electro-Fenton for the reduction of the environmental impact of antibiotics, *Sep. Purif. Technol.* 276 (2021).
- [31] J.F. Pérez, J. Llanos, C. Sáez, C. López, P. Cañizares, M.A. Rodrigo, Development of an innovative approach for low-impact wastewater treatment: a microfluidic flow-through electrochemical reactor, *Chem. Eng. J.* 351 (2018) 766–772.
- [32] M. Herraiz-Carboné, S. Cotillas, E. Lacasa, P. Cañizares, M.A. Rodrigo, C. Sáez, Enhancement of UV disinfection of urine matrixes by electrochemical oxidation, *J. Hazard. Mater.* 410 (2021).
- [33] M. Herraiz-Carboné, E. Lacasa, S. Cotillas, M. Vasileva, P. Cañizares, M.A. Rodrigo, C. Sáez, The role of chloramines on the electrodisinfection of *Klebsiella pneumoniae* in hospital urines, *Chem. Eng. J.* 409 (2021).
- [34] S. Cotillas, E. Lacasa, C. Sáez, P. Cañizares, M.A. Rodrigo, Removal of pharmaceuticals from the urine of polymedicated patients: a first approach, *Chem. Eng. J.* 331 (2018) 606–614.
- [35] J. Dupont, F. Dumont, C. Menanteau, M. Pommepuy, Calibration of the impedance method for rapid quantitative estimation of *Escherichia coli* in live marine bivalve molluscs, *J. Appl. Microbiol.* 96 (2004) 894–902.
- [36] S. Zhu, S. Schnell, M. Fischer, Rapid detection of *Cronobacter* spp. with a method combining impedance technology and rRNA based lateral flow assay, *Int. J. Food Microbiol.* 159 (2012) 54–58.
- [37] K.A. Alexander, C.E. Sanderson, M.H. Larsen, S. Robbe-Austerman, M.C. Williams, M.V. Palmer, Emerging tuberculosis pathogen hijacks social communication behavior in the group-living banded mongoose (*Mungos mungo*), *MBio* 7 (2016).
- [38] K.L. Nielsen, P. Dynesen, P. Larsen, L. Jakobsen, P.S. Andersen, N. Frimodt-Møller, Role of urinary cathelicidin LL-37 and human β -defensin 1 in uncomplicated *Escherichia coli* urinary tract infections, *Infect. Immun.* 82 (2014) 1572–1578.
- [39] M. Herraiz-Carboné, S. Cotillas, E. Lacasa, M. Vasileva, C. Sainz de Baranda, E. Riquelme, P. Cañizares, C. Sáez, Disinfection of polymicrobial urines by electrochemical oxidation: removal of antibiotic-resistant bacteria and genes, *J. Hazard. Mater.* 426 (2022), 128028.
- [40] Z.M. Jaafar, M.A. Dhahi, A.K.H. Abd, S.M. Jaafar, Molecular identification and antibiotics resistance genes profile of *Pseudomonas aeruginosa* isolated from Iraqi patients, *Afr. J. Microbiol. Res.* 8 (2014) 2183–2192.
- [41] D. Bibbal, V. Dupouy, J.-P. Ferré, P.-L. Toutain, O. Fayet, M.-F. Prère, A. Bousquet-Mélou, Impact of three ampicillin dosage regimens on selection of ampicillin resistance in enterobacteriaceae and excretion of bla TEM genes in swine feces, *Appl. Environ. Microbiol.* 73 (2007) 4785–4790.
- [42] A.V. Wilpert, Über die Analyse von Hypochlorit und Chlorit in einer Lösung, *Z. Anal. Chem.* 155 (1957), 378–378.
- [43] H. Freytag, Zur bestimmung von hypochlorit, chlorid und chlorat in chlorkalk, *Z. Anal. Chem.* 171 (1959), 458–458.
- [44] A. WPCF, APHA, Standard Methods for the Examination of Water and Wastewater, 20th Ed, American Public Health Association (APHA), Washington DC, 1998.
- [45] G. Eisenberg, Colorimetric determination of hydrogen peroxide, *Ind. Eng. Chem. Anal. Ed.* 15 (1943) 327–328.
- [46] W. Wu, Y. Feng, G. Tang, F. Qiao, A. McNally, Z. Zong, NDM metallo- β -lactamases and their bacterial producers in health care settings, *Clin. Microbiol. Rev.* 32 (2019) e00115-00118.
- [47] M. Gajdác, The continuing threat of methicillin-resistant *Staphylococcus aureus*, *Antibiotics* 8 (2019).
- [48] Y. Guo, G. Song, M. Sun, J. Wang, Y. Wang, Prevalence and therapies of antibiotic-resistance in *Staphylococcus aureus*, *Front. Cell. Infect. Microbiol.* 10 (2020).
- [49] J. Berman, D.J. Krysan, Drug resistance and tolerance in fungi, *Nat. Rev. Microbiol.* 18 (2020) 319–331.
- [50] A. Kumar, H.P. Schweizer, Bacterial resistance to antibiotics: active efflux and reduced uptake, *Adv. Drug Deliv. Rev.* 57 (2005) 1486–1513.
- [51] J. Blair, M.A. Webber, A.J. Baylay, D.O. Ogbolu, L.J. Piddock, Molecular mechanisms of antibiotic resistance, *Nat. Rev. Microbiol.* 13 (2015) 42–51.
- [52] W.C. Reygaert, An overview of the antimicrobial resistance mechanisms of bacteria, *AIMS Microbiol.* 4 (2018) 482–501.
- [53] A. Ghasemnejad, M. Doudi, N. Amirzofari, The role of the blaKPC gene in antimicrobial resistance of *Klebsiella pneumoniae*, *Iran. J. Microbiol.* 11 (2019) 288–293.
- [54] T. Essayagh, A. Karimou, S. Elhamzaoui, Carbapenemases among *Klebsiella pneumoniae*: sensitivity, E-test and Hodge test, *Ann. Biol. Clin.* (2012) 299–304.
- [55] D. Girlich, T. Naas, P. Nordmann, Biochemical characterization of the naturally occurring oxacillinase OXA-50 of *Pseudomonas aeruginosa*, *Antimicrob. Agents Chemother.* 48 (2004) 2043–2048.
- [56] C.L.C. Wielders, A.C. Fluit, S. Brisse, J. Verhoef, F.J. Schmitz, mecA gene is widely disseminated in *Staphylococcus aureus* population, *J. Clin. Microbiol.* 40 (2002) 3970–3975.
- [57] T. Ito, K. Hiramatsu, Acquisition of methicillin resistance and progression of multiantibiotic resistance in methicillin-resistant *Staphylococcus aureus*, *Yonsei Med. J.* 39 (1998) 526–533.
- [58] J.F. Pérez, S. Sabatino, A. Galia, M.A. Rodrigo, J. Llanos, C. Sáez, O. Scialdone, Effect of air pressure on the electro-Fenton process at carbon felt electrodes, *Electrochim. Acta* 273 (2018) 447–453.
- [59] Y. Jiao, L. Ma, Y. Tian, M. Zhou, A flow-through electro-Fenton process using modified activated carbon fiber cathode for orange II removal, *Chemosphere* 252 (2020), 126483.
- [60] W.R.P. Barros, T. Ereno, A.C. Tavares, M.R.V. Lanza, In situ electrochemical generation of hydrogen peroxide in alkaline aqueous solution by using an unmodified gas diffusion electrode, *ChemElectroChem* 2 (2015) 714–719.
- [61] L.E. Murdoch, L. Bailey, E. Banham, F. Watson, N.M.T. Adams, J. Chewins, Evaluating different concentrations of hydrogen peroxide in an automated room disinfection system, *Lett. Appl. Microbiol.* 63 (2016) 178–182.
- [62] E. Petrucci, A. Da Pozzo, L. Di Palma, On the ability to electrogenerate hydrogen peroxide and to regenerate ferrous ions of three selected carbon-based cathodes for electro-Fenton processes, *Chem. Eng. J.* 283 (2016) 750–758.
- [63] J.C. Crittenden, R.R. Trussell, D.W. Hand, K.J. Howe, G. Tchobanoglous, *MWH's Water Treatment: Principles and Design*, John Wiley & Sons, 2012.
- [64] M. Herraiz-Carboné, S. Cotillas, E. Lacasa, P. Cañizares, M.A. Rodrigo, C. Sáez, Removal of antibiotic resistant bacteria by electrolysis with diamond anodes: a pretreatment or a tertiary treatment? *J. Water Process Eng.* 38 (2020).
- [65] E.A. Curling, M.J. McKie, L. Meter, B. Saunders, S.A. Andrews, R.C. Andrews, Estimation of chloramine decay in drinking water distribution systems, *J. Water Process Eng.* 46 (2022), 102558.
- [66] S. Kinani, B. Richard, Y. Souissi, S. Bouchonnet, Analysis of inorganic chloramines in water, *TrAC Trends Anal. Chem.* 33 (2012) 55–67.
- [67] M. Herraiz-Carboné, E. Lacasa, S. Cotillas, M. Vasileva, P. Cañizares, M.A. Rodrigo, C. Sáez, The role of chloramines on the electrodisinfection of *Klebsiella pneumoniae* in hospital urines, *Chem. Eng. J.* 409 (2021), 128253.
- [68] S. Cotillas, D. Clematis, P. Cañizares, M.P. Carpanese, M.A. Rodrigo, M. Panizza, Degradation of dye procion red MX-5B by electrolytic and electro-irradiated technologies using diamond electrodes, *Chemosphere* 199 (2018) 445–452.
- [69] H. Rubí-Juárez, S. Cotillas, C. Sáez, P. Cañizares, C. Barrera-Díaz, M.A. Rodrigo, Use of conductive diamond photo-electrochemical oxidation for the removal of pesticide glyphosate, *Sep. Purif. Technol.* 167 (2016) 127–135.
- [70] M.J.M. de Viales, C. Sáez, J.F. Pérez, S. Cotillas, J. Llanos, P. Cañizares, M. A. Rodrigo, Irradiation-assisted electrochemical processes for the removal of persistent organic pollutants from wastewater, *J. Appl. Electrochem.* 45 (2015) 799–808.
- [71] E. Lacasa, P. Cañizares, J. Llanos, M.A. Rodrigo, Effect of the cathode material on the removal of nitrates by electrolysis in non-chloride media, *J. Hazard. Mater.* 213–214 (2012) 478–484.
- [72] J.M. Bockris, J. Kim, Electrochemical treatment of low-level nuclear wastes, *J. Appl. Electrochem.* 27 (1997) 623–634.
- [73] E. Lacasa, P. Cañizares, J. Llanos, M.A. Rodrigo, Removal of nitrates by electrolysis in non-chloride media: effect of the anode material, *Sep. Purif. Technol.* 80 (2011) 592–599.
- [74] K.A. Thorn, L.G. Cox, Ultraviolet irradiation effects incorporation of nitrate and nitrite nitrogen into aquatic natural organic matter, *J. Environ. Qual.* 41 (2012) 865–881.
- [75] F. Soltermann, T. Widler, S. Canonica, U. von Gunten, Photolysis of inorganic chloramines and efficiency of trichloramine abatement by UV treatment of swimming pool water, *Water Res.* 56 (2014) 280–291.
- [76] J. Li, E.R. Blatchley III, UV photodegradation of inorganic chloramines, *Environ. Sci. Technol.* 43 (2009) 60–65.
- [77] R. Yin, E.R. Blatchley, C. Shang, UV photolysis of mono- and dichloramine using UV-LEDs as radiation sources: photodecay rates and radical concentrations, *Environ. Sci. Technol.* 54 (2020) 8420–8429.